Results in Physics 7 (2017) 2575–2581

Contents lists available at ScienceDirect

Results in Physics

journal homepage: www.journals.elsevier.com/results-in-physics

Bell's twin rockets non-inertial length enigma resolved by *real* geometry

Brian Coleman *

BC Systems (Erlangen)—Velchronos, Ballinakill Bay, Moyard, County Galway, Ireland

ARTICLE INFO

Article history:
Received 22 May 2017
Accepted 6 July 2017
Available online 12 July 2017

Keywords:
Homogeneous acceleration
Non-inertial length
Radar intervals
Real-values metric
Minkowski metric
Photon crossing rate
Hemix
Hemicoid

ABSTRACT

A priori uniformity and monotonicity of the 'non-inertial length' expansion of a uniformly co-accelerating medium, uniquely yield an unfamiliar *'hemicoid'* real-values metric surface Υ in $\mathbb{R}^3$. $\Upsilon(\tau, l)$ hosts congruent helicoidally distributed fixed-l *'hemix world-lines'* tracing medium increments' clock times τ and crossed by fixed-τ medium helices of parameterized length λ sharing comoving 'non-inertial frames'. Radar intervals and expansion factor $\partial\lambda/\partial l = \sqrt{(1 + v^2/c^2)}$ conform to requirements established in *Coleman, Results in Physics, **6**, 2016—Minkowski spacetime does not apply to a homogeneously accelerating medium*. Co-directional radar paths on Υ mapped from home frame chart diagonals crossing hyperbolic world-lines, surf 'horizon' increment hemices, whereas counter-directional radar paths tend to 'overlap' horizon medium helices. They also traverse each medium expansion helix at respectively identical angles and geodesic curvatures, independently of differing rocket emission times. Surface Υ's real metric is: $ds^2 = d\tau^2 + d\lambda^2 + \left[2\tanh\tau.(\tanh\tau - 1/\cosh\tau)/\sqrt{(1 + \tanh^2\tau)}\right] d\tau.d\lambda$.

1. Introduction

In 1987 an *American Journal of Physics* paper [5], relating to an earlier paper [3] in that journal, roundly castigated relativity literature attempts to resolve the 'own-length'[1] of a co-accelerating medium between identical twin rockets[2] (as also recalled in [17]):

> "The approach is unnecessarily formal or abstract, key concepts are left undefined, a working knowledge of general relativity is assumed, no attempt is made to give a physical interpretation of the coordinates introduced, the relationship between different sets of coordinates used is not made, and no investigation of the properties of the frame is made."

This still ongoing state of affairs was unwittingly exemplified by [5]'s own failure, in spite of its concerted efforts and *a two year journal review period*, to arrive at a feasible solution based on inter-rocket radar intervals *presumed—wrongly—to be constant* (⇒ Fig. 2, Eq. (13) below and [17]). The same issue had been addressed in 1976, likewise inconclusively, by *John Bell* [4] who nevertheless famously exposed diverse opinions among his Geneva CERN colleagues on this supposedly clearcut topic. The widely held simplistic 'inverse contraction' γ expansion factor claimed for example in [7,8], applies only *after* both rockets cease accelerating (⇒[17,13]).

In 2004 *Brown and Pooley* [6][3] wrote: *"It is argued that Minkowski spacetime cannot serve as the deep structure within a "constructive" version of the special theory of relativity, contrary to widespread opinion in the philosophical community."* A more explicit challenge appeared in 2010 in a Moscow English language journal [10]: *"The standard solution of Bell's well-known problem…must be revised"*. In a 2014 paper [12],[4] the latter's authors very aptly stated *"The [Bell's] paradox is solved only when going out of [abandoning] the Minkowski [complex variables] space to the Riemann [real variables] space"*, and proposed ([12] p.24) a length formula equivalent[5] to

$$\Lambda(\tau) = \ln(\cosh L + \sinh L \cosh\tau). \tag{1}$$

Yet they also claimed that *"…all authors (except [own papers] [3–5]) connect the string rupture with the Lorentz shrinkages"*, in spite of having acknowledged in 2009 a direct communication of the present author's different *non-presentism* equation

$$\Lambda(\tau) = L\sqrt{1 + \tanh^2\tau} = L\sqrt{1 + v^2/c^2}. \tag{2}$$

* Corresponding author.
E-mail address: brian.coleman.velchron@gmail.com

[1] Discarding the relativisically dysfunctional adjective 'proper'.

[2] This topic is often referred to as *Bell's string paradox* or *Bell's spaceship paradox*.

[3] *Minkowski spacetime: a glorious non-entity* http://philsci-archive.pitt.edu/1661/1/Minkowski.pdf.

[4] http://wireilla.com/physics/ijrap/papers/3114ijrap04.pdf.

[5] Using the present paper's notation, L is the scaled 'launch' length, and τ the rockets' scaled own-time.

http://dx.doi.org/10.1016/j.rinp.2017.07.013
2211-3797/

This 2009 formula also appeared in the web abstract [11][6] of a 2012 *Deutsche Physikalische Gesellschaft* presentation in Göttingen likewise not referred to in a 2017 open access paper [18][7] which, moreover, overlooked the clearcut radar approach to the 'rigid motion' acceleration topic expounded in the present author's 2016 paper [17][8] referencing the 2012 abstract. Significantly, those physicists' 2017 paper overruled their own above earlier Eq. (1): *"Although the formula… is correct both for large and low accelerations, it does not solve the Bell paradox in principle."* ([18] p.16).

The solution to the hitherto unresolved extended accelerating medium issue[9] involves a *real-values metric* surface Υ uniformly and monotonically expanding laterally in accordance with Eq. (2). Crucially, this surface hosts bidirectional radar trajectories whose intervals and boundary conditions match those already established in [17].

2. The missing unit thrust own-surface

A simple question apparently not addressed even in geometry literature is:

> Is there any way a flexible flat rectangular strip may be transformed to a smooth and regular open surface so that lateral lines increase in length *as well as in curvature* both uniformly and monotonically?

Should such a surface $\Upsilon(\tau, l)$ exist ($0 \leqslant l \leqslant L$), it conceivably may represent a homogeneously accelerating extended medium by hosting fixed-τ *medium curves* of expanding parameterized length[10] λ crossed at equal intervals by congruent fixed-l *increment curves* whose path lengths trace each increment's own-time τ. As expansion factor $\partial\lambda/\partial l = \varepsilon(\tau)$ must be uniform along each fixed own-time medium curve and must monotonically increase with own-time τ, it follows that fixed-l curves must be *helicoidally spread* and fixed-τ curves must be *axially concentric helices* reflecting the medium's ever increasing *'own-length'* $\Lambda = L.\varepsilon(\tau)$. The familiar multi-level car parking driveway has helicoidally distributed radial lines and concentric helices increasing in length with cylindrical radius r. Their helices' *curvatures* however (⇒ Eq. (34)) increase with r only up to $r = 1/m$ (m being the helicoid's fixed inverse pitch) and thereafter *decrease*.

As it turns out, if we not only limit the *cylindrical radius* of the helicoid's (thereby *nonplanar*) generator curve to within $1/m$, but also require its *longitude* and *spherical radius* coordinates to be monotonic so that the generated helicoid is free of all topological inflections, a 'hemicoid' surface Υ *uniquely* emerges whose 'hemix' generator curve, though seemingly hitherto unknown, has two simple defining characteristics: *The hemix is a hemispherical curve whose path length increases in accordance with its traversed longitude.* This is unequivocally established in the paper's Appendix.

$$\text{Unit thrust own-surface } \Upsilon(\tau, l) = \left[\tanh\tau\cos(\tau+l), \tanh\tau\sin(\tau+l), \frac{1}{\cosh\tau} + l\right]. \tag{3}$$

$$\Upsilon_\tau = \frac{\partial\Upsilon}{\partial\tau} = \left[\frac{\cos(\tau+l)}{\cosh^2\tau} - \tanh\tau\sin(\tau+l), \frac{\sin(\tau+l)}{\cosh^2\tau} + \tanh\tau\cos(\tau+l), \frac{-\sinh\tau}{\cosh^2\tau}\right]. \tag{4}$$

As expected, increment curves' path length speed $\left|\frac{\partial\Upsilon}{\partial\tau}\right| = \sqrt{\Upsilon_\tau \cdot \Upsilon_\tau} = 1$.

Expansion $\frac{\partial\lambda}{\partial l}$ equals the modulus of each fixed-τ medium helix's tangent.

$$\Upsilon_l = \frac{\partial\Upsilon}{\partial l} = [-\tanh\tau\sin(\tau+l), \tanh\tau\cos(\tau+l), 1]. \tag{5}$$

$$\text{Unit thrust non-inertial expansion } \varepsilon(\tau) = \frac{\partial\lambda}{\partial l} = \left|\frac{\partial\Upsilon}{\partial l}\right| = \sqrt{1+\tanh^2\tau}. \tag{6}$$

Equations for metric surface Υ's increment and medium curves are obtained by adopting *fixed values* of l and τ respectively in Eq. (3).[11] Fig. 1's 'hemicoid' own-surface Υ shows lateral medium helices sharing own-τ-time where $0 \leqslant \tau \leqslant 3\pi/2$ i.e. for rocket scaled speed range $0 \leqslant v \leqslant \tanh(3\pi/2)$.

The resulting open surface not only meets the radar path conditions summarised in this paper's abstract, in addition to characterising uniform and monotonic non-inertial own-length increase, its evolved hemix generator curve also happens to geometrically epitomise a fixed thrust rocket's well established familiar relativistic parameters.

3. Unit thrust rockets radar trajectories

Recapitulating parts of [17], a fixed thrust rocket home frame's velocity v, time t and distance x travelled under acceleration, as well as its own-time τ, are all *zero* at launch. Scaling time so that limit speed c is *one* and length so the rocket's constant own-acceleration α is also one, the familiar scaled equations are (⇒[17] page 32):

$$t = \sinh\tau; \quad x = \cosh\tau - 1;$$
$$v = \tanh\tau; \quad (x+1)^2 - t^2 = 1. \tag{7}$$

Bearing in mind that inertial length is defined in terms of *electromagnetic wavelengths*, we also recall the Gedankenexperiment described in [17]'s section *Photon crossing rates*. An emitted radar photon's encountered[12] rocket own-time on emission is designated as $\acute{\tau}$, on reflection as $\hat{\tau}$ and on return as $\grave{\tau}$. Variables τ, t and x *without an accent*, denote values of *an arbitrary intermediate increment* ($0 < l < L$) encountered by the photon. Rocket and (imagined) increment clocks are zeroed at launch.

3.1. Outgoing radar paths

Referring to Fig. 2, for a photon emitted from the rear rocket at rear rocket own-time $\acute{\tau} = \sinh^{-1}\acute{t}$ i.e. at home-frame time $\acute{t} = \sinh\acute{\tau}$, the rear rocket will have travelled under acceleration to a home-frame position $\acute{x} = \cosh\acute{\tau} - 1$. The same photon subsequently arrives at an arbitrary increment l at the latter's own-time $\tau = \sinh^{-1}t$, i.e. at home-frame time $t = \sinh\tau$ when increment l has a home-frame position $x + l = \cosh\tau - 1 + l$. The photon

[6] http://www.dpg-verhandlungen.de/year/2012/conference/goettingen/part/gr/session/4/contribution/4.

[7] http://www.journalrepository.org/media/journals/PSIJ_33/2017/Jan/Podosenov1322016PSIJ30616.pdf.

[8] http://www.sciencedirect.com/science/article/pii/S2211379716000024 [17]'s minor (improved) corrigendum: Page 34: The inital words "fixed own-time" should be deleted. Two lines after Eq. (19): "identical own-times" should read "identical velocities". Eight lines from page 37's end, "clock own-times" should be replaced by "home frame times".

[9] As alluded to in [17], each medium increment is assumed to have its own 'minuscule rocket'.

[10] λ being each increment l's respective non-inertial own-length from the medium's rear end.

[11] Fig. 1's actual diagram, created using software based on PoVRay [15], was first presented in an unsuccessful 2009 submission to the *American Journal of Physics*—AJP manuscript MS23122.

[12] Radar signals use wave pulses rather than photons—a descriptively useful 'equivalent'.

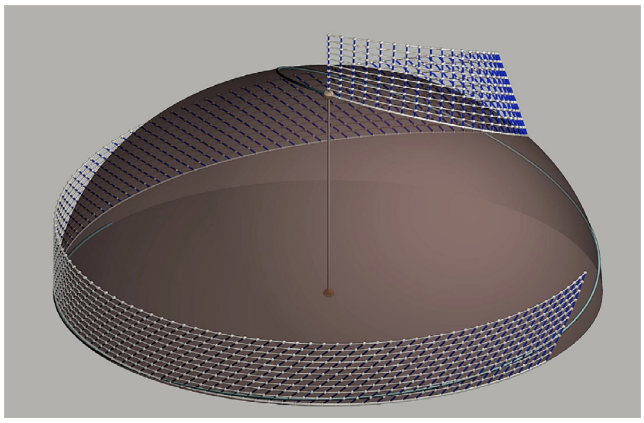

Fig. 1. Unit thrust own-surface with fixed-l increment curves and fixed-τ medium curves.

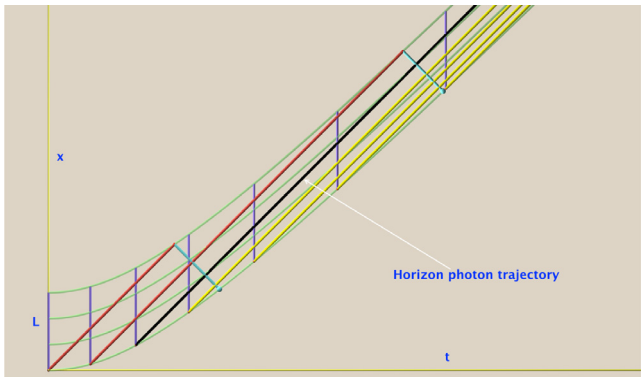

Fig. 2. Home frame world-surface of a uniformly accelerating medium, with reflected and nonreflected radar trajectories and fixed velocity loci at regular $\Delta\tau$ periods.

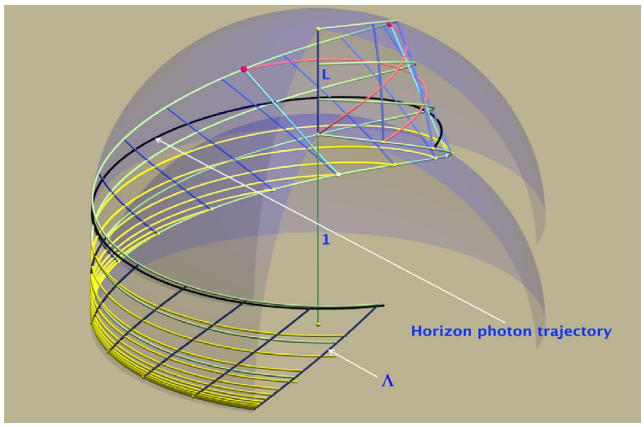

Fig. 3. Unit thrust own-surface with increment and medium curves and radar trajectories.

travels at unit speed in the home frame so $(x+l-\acute{x}) = (t-\acute{t})$ i.e. $\cosh\tau - 1 + l - (\cosh\acute{\tau} - 1) = \sinh\tau - \sinh\acute{\tau}$.

OUTGOING PHOTON EQUATIONS

$$l = -e^{-\tau} + e^{-\acute{t}} \qquad i.e. \qquad \frac{\partial l}{\partial \tau} = e^{-\tau}. \tag{8}$$

With $\hat{\tau}$ as the front rocket's reflection time where $l = L$:

$$e^{-\acute{t}} = e^{-\hat{\tau}} + L \qquad i.e. \qquad e^{\hat{\tau}} = \frac{1}{e^{-\acute{t}} - L}. \tag{9}$$

From (9)ii, for a photon whose emission time is $\acute{\tau} = \ln(\frac{1}{L})$, $e^{\hat{\tau}} = \infty$. As a medium's shared own-time τ approaches ∞ and the medium approaches unit limit speed in the inertial home frame, the 'horizon photon' trajectory (in black) thus tends to *'surf'* the front rocket i.e. get ever closer to it at nearly zero speed, without ever reaching it. Later photons surf respective *intermediate* medium increments.

For an outgoing photon's radar formula ρ, we turn to radar transit Eq. (8)i for a photon's rear rocket emission own-time $\acute{\tau}$ and replace l with $-e^{-\tau} + e^{-\acute{t}}$ in (3):

$$\rho = \left[\tanh\tau\cos(\tau - e^{-\tau} + e^{-\acute{\tau}}), \tanh\tau\sin(\tau - e^{-\tau} + e^{-\acute{\tau}}), \frac{1}{\cosh\tau} - e^{-\tau} + e^{-\acute{t}}\right]. \tag{10}$$

3.2. Returning radar paths

A reflected photon whose emission time $\acute{\tau} < \ln(1/L)$,[13] travels *backwards* to meet an arbitrary increment l at home time $t = \sinh\tau$ and home *position* $x + l = \cosh\tau - 1 + l$, over equal home time and distance intervals:[14] $t - \hat{t} = (\hat{x} + L) - (x + l)$. Therefore $\sinh\tau - \sinh\hat{\tau} = (\cosh\hat{\tau} - 1 + L) - (\cosh\tau - 1 + l)$ i.e. $e^{\tau} - e^{\hat{\tau}} = L - l$ and from (9)ii:

RETURNING PHOTON EQUATIONS l

$$= -e^{\tau} + L + 1/(e^{-\acute{t}} - L) \; i.e. \; \frac{\partial l}{\partial \tau} = -e^{\tau}. \tag{11}$$

Replacing this l value in (3) gives us *the returning photon's radar equation*. For the rear rocket $l = 0$ and $\tau = \grave{\tau}$. Hence, using (11)i:

$$e^{\grave{\tau}} = L + 1/(e^{-\acute{t}} - L). \tag{12}$$

REAR ROCKET RADAR INTERVAL $\grave{\tau} - \acute{\tau} = \ln\left[L + \frac{1}{e^{-\acute{t}} - L}\right] - \acute{\tau}.$ (13)

Since from (9)ii $e^{\hat{\tau}} = 1/(e^{-\acute{t}} - L)$, for a *returned* photon (12) yields:

$$\grave{\tau} - \hat{\tau} = \ln\left[L + \frac{1}{e^{-\acute{t}} - L}\right] - \ln\left[\frac{1}{e^{-\acute{t}} - L}\right] = \ln\left[\frac{L + \frac{1}{e^{-\acute{t}} - L}}{\frac{1}{e^{-\acute{t}} - L}}\right] = \ln\left[L(e^{-\acute{t}} - L) + 1\right]. \tag{14}$$

Thus for $e^{-\acute{t}}$ very close to L, $\grave{\tau} - \hat{\tau} \approx \ln(1) = 0$. For an emission time $\acute{\tau}$ near horizon value $\ln 1/L$, a photon's returning unit thrust medium's traversing time tends towards zero. In such a case, as τ approaches ∞, a *counter-directional* reflected photon would traverse the medium at a virtually infinite 'crossing rate'. In Fig. 2 (paper [17]'s Fig. 2) and Fig. 3, for the chosen 'launch length' L and emission interval $\Delta\tau$ period the first two photons emitted are reflected. Their trajectories appear in red.

Crucially, surface Υ's medium curves' expansion $\varepsilon(\tau) = \frac{\partial\lambda}{\partial\tau}$ is monotonic and complies with the respective necessary forward and reverse photon medium-timed crossing rate conditions foreseen in [17] (that paper's page 37 Eqs. (32) and (33)):

$$\text{Forward rate } \frac{\partial\lambda}{\partial\tau} = \frac{\partial\lambda}{\partial l}\cdot\frac{\partial l}{\partial\tau} = \sqrt{1 + \tanh^2\tau}\cdot e^{-\tau} \text{ hence } \left.\frac{\partial\lambda}{\partial\tau}\right|_{\tau\to\infty} = 0. \tag{15}$$

[13] i.e. $e^{\acute{\tau}} < 1/L$. Otherwise the photon never reaches the front rocket.
[14] $\hat{x} + L$ being the front rocket's position as the photon is reflected.

$$\text{Reverse rate } -\frac{\partial\lambda}{\partial\tau} = -\frac{\partial\lambda}{\partial l}\cdot\frac{\partial l}{\partial\tau} = \sqrt{1+\tanh^2\tau}\cdot e^{\tau} \text{ hence } -\left.\frac{\partial\lambda}{\partial\tau}\right|_{\tau\to\infty} = \infty. \quad (16)$$

3.3. Shared radar curves' crossing angles and geodesic curvatures

τ-differentiating radar curve (10) gives us tangent vector ρ_τ and modulus $|\rho_\tau|$:

$$\rho_\tau = \left[\frac{1}{\cosh^2\tau}\cos(\tau - e^{-\tau} + e^{-\acute{t}}) - \tanh\tau(1+e^{-\tau})\sin(\tau - e^{-\tau} + e^{-\acute{t}}),\right.$$
$$\frac{1}{\cosh^2\tau}\sin\left(\tau - e^{-\tau} + e^{-\acute{t}}\right) + \tanh\tau(1+e^{-\tau})\cos\left(\tau - e^{-\tau} + e^{-\acute{t}}\right),$$
$$\left.\frac{-\sinh\tau}{\cosh^2\tau} + e^{-\tau}\right]. \quad (17)$$

$$|\rho_\tau|^2 = \frac{1}{\cosh^4\tau} + \tanh^2\tau.(1+e^{-\tau})^2 + \left(\frac{-\sinh\tau}{\cosh^2\tau} + e^{-\tau}\right)^2. \quad (18)$$

Replacing l with $-e^{-\tau} + e^{-\acute{t}}$ in increment curve and medium curve tangent vector Eqs. (4) and (5), we obtain for Υ_l and Υ_τ:

$$\Upsilon_l = \left[-\tanh\tau\sin(\tau - e^{-\tau} + e^{-\acute{t}}), \tanh\tau\cos(\tau - e^{-\tau} + e^{-\acute{t}}), 1\right]. \quad (19)$$

$$\Upsilon_\tau = \left[\frac{\cos(\tau - e^{-\tau} + e^{-\acute{t}})}{\cosh^2\tau} - \tanh\tau\sin(\tau - e^{-\tau} + e^{-\acute{t}}),\right.$$
$$\left.\frac{\sin(\tau - e^{-\tau} + e^{-\acute{t}})}{\cosh^2\tau} + \tanh\tau\cos(\tau - e^{-\tau} + e^{-\acute{t}}), \frac{-\sinh\tau}{\cosh^2\tau}\right]. \quad (20)$$

Since $|\Upsilon_\tau| = 1$ and $|\Upsilon_l| = \sqrt{1+\tanh^2\tau}$, (17)–(20) yield (using MAPLE [14]):

RADAR/MEDIUM CURVES EMISSION TIME-INDEPENDENT CROSSING COSINE

$$\frac{\rho_\tau\cdot\Upsilon_l}{|\rho_\tau||\Upsilon_l|} = \frac{(1+\tanh^2\tau)e^{-\tau} + \tanh^2\tau - \tanh\tau/\cosh\tau}{\sqrt{\frac{1}{\cosh^4\tau} + \tanh^2\tau.(1+e^{-\tau})^2 + \left(\frac{-\sinh\tau}{\cosh^2\tau} + e^{-\tau}\right)^2}.\sqrt{1+\tanh^2\tau}}. \quad (21)$$

Expression (21) reduces to $1/\sqrt{2}$ (45 degrees cosine) for $\tau = 0$ and likewise as $\tau \to \infty$. As is also evident in Fig. 3, radar trajectories are thus initially diagonal to fixed-τ medium and fixed-l increment curves, in accordance with unit limit speed in the rocket's launch home frame. As likewise expected, non-reflected photon trajectories ultimately 'surf' increment curves.

A particularly notable parameter is radar trajectories' *geodesic curvature* on surface Υ. Geodesic curvature equals the dot product of Υ's *normal unit vector* $\frac{\Upsilon_\tau\times\Upsilon_l}{|\Upsilon_\tau|.|\Upsilon_l|}$ with the cross product of the radar trajectory's *tangent vector* ρ_τ and it's *'acceleration vector'* $\rho_{\tau\tau}$ (not listed) divided by the tangent vector's modulus cubed (⇒[9] p.169).

3.4. A 'retrospective' insight

Although vectors $\Upsilon_\tau, \Upsilon_l, \rho_\tau$ and $\rho_{\tau\tau}$ each contain radar emission time expressions $e^{-\acute{t}}$, this term *is cancelled out* in angle cosine Eq. (21) as well as in geodesic curvature expression (22). Successive radar trajectories on own-surface Υ cross each shared own-time medium helix at respectively identical angles and with identical geodesic curvatures, independently of the photons' differing rear rocket emission times. This, 'in hindsight', constitutes *a necessary physics condition*, since the spatio-temporal characteristics of a photon's crossing of an extended accelerating medium, whatever they might be, would not in any way depend on the emitting rocket clock's own-time $\acute{t}$.

4. The uniform thrust medium's real metric

From Υ's Eq. (3), $r = \tanh\tau, \theta = \tau + l$ and $z = 1/\cosh\tau + l$ i.e. $dr = \frac{1}{\cosh^2\tau}d\tau$, $d\theta = d\tau + dl$ and $dz = \frac{-\sinh(\tau)}{\cosh^2\tau}d\tau + dl$. Υ's metric $ds^2_\Upsilon = dr^2 + r^2d\theta^2 + dz^2$ becomes

$$ds^2_\Upsilon = d\tau^2 + (1+\tanh^2\tau)dl^2 - 2\frac{\sinh\tau}{\cosh^2\tau}(1-\sinh\tau)d\tau dl$$

which gives us (since $\frac{\partial\lambda}{\partial l} = \sqrt{1+\tanh^2\tau}$):

THE UNIT THRUST MEDIUM'S OWN-SURFACE METRIC ds^2_Υ

$$= d\tau^2 + d\lambda^2 + 2\tanh\tau\left(\frac{\tanh\tau - 1/\cosh\tau}{\sqrt{1+\tanh^2\tau}}\right)d\tau.d\lambda. \quad (23)$$

Significantly, because of its nonzero mixed $d\tau.d\lambda$ term, metric (23) is *wholly incompatible* with the Minkowski spacetime interval $ds^2_{\mathfrak{M}} = d\tau^2 - d\lambda^2 = 0$. This is a firm indication that *Minkowski spacetime is not generally valid in special relativity*—as already intimated in several papers referred to in the INTRODUCTION.

5. Conclusions

- With no relativistic pre-assumptions, the unique laterally expanding $\lambda|\tau$ real metric 'own-surface' Υ *independently* emerges solely from expected characteristics of *uniformity*, *monotonicity* and *regularity*. This 'hemicoid' surface Υ and its hemispherical generator 'hemix' curve—which is curiously reminiscent of *Pedro Nuñes*' 1537 *loxodromes* used for centuries in navigation, are to all appearances unknown both in physics and as well as in geometry literature.[15]
- Surface Υ's uniqueness constitutes a 'by default' accelerating frame length expansion criterion hitherto categorically missing from relativity theory. No external 'action principle' is needed which would have entailed asymmetrical inter-increment forces and time delays and anyhow is *superfluous* for the primary purpose of establishing an idealised uniformly expanding non-inertial length.
- The seemingly unknown hemix's multiple properties are perhaps worthy of mention. Its colatitude equals the *Gudermannian* of its equal path length and traversed longitude. Colatitude also equals the curve's meridianal inclination whose *sine* equals *the*

RADAR CURVES EMISSION TIME-INDEPENDENT GEODESIC CURVATURE κ_G

$$= \frac{\Upsilon_\tau\times\Upsilon_l}{1.|\Upsilon_l|}\cdot\frac{\rho_\tau\times\rho_{\tau\tau}}{|\rho_\tau|^3} = \frac{\sinh\tau(2\cosh^2\tau-1)e^{-3\tau} + ((3\sinh\tau-3)\cosh^2\tau - 3\sinh\tau + 3)e^{-2\tau} + (4 - \cosh^5\tau + \cosh^4\tau - 2\sinh\tau\cosh^3\tau + (3\sinh\tau-5)\cosh^2\tau + 2\sinh\tau\cosh\tau)e^{-\tau} + \cosh^2\tau(\cosh^2\tau + 2\sinh\tau - 2)}{\sqrt{\cosh^4\tau + 2\cosh^2\tau\sinh\tau - 2\sinh\tau}\left(\sqrt{(2\cosh^2\tau-1)e^{-2\tau} + 2\sinh\tau(\sinh\tau-1)e^{-\tau} + \cosh^2\tau)}\right)^3}. \quad (22)$$

[15] The writer would much appreciate notification of any previous references to this multifarious curve.

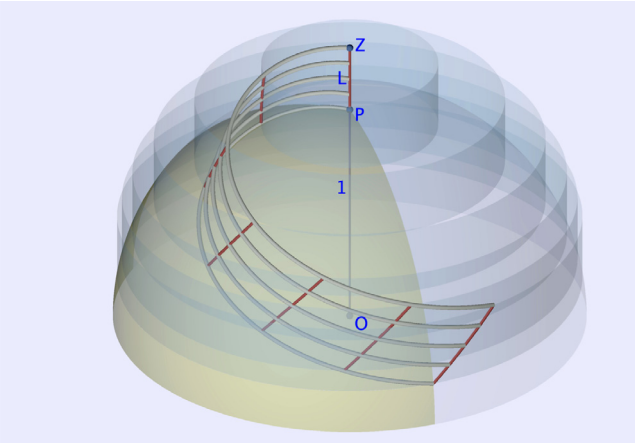

Fig. 4. Schematic helicoid Υ, surface of revolution W_0 and helices' cylinders V_τ.

medium's increasing scaled velocity i.e. $v = \sin\phi$. This particularly significant parameter corresponds to the scaled angle introduced in Uruguay-born Argentinian physicist *Enrique Loedel's* 1948 *symmetrical spacetime chart* [1] and often used in relativity literature. The hemix's geodesic curvature on its hemisphere equals twice its elevation and its 'natural equations' (independent of position and orientation[16]) defining the curve in terms of *curvature* κ and *torsion* η are:

$$\eta = \frac{1}{2}\sqrt{\left(\frac{1}{\kappa^2}-1\right)\left(\frac{5}{\kappa^2}-1\right)} \text{ i.e. } \kappa^2 = \frac{3-2\sqrt{1+5\eta^2}}{1-4\eta^2}. \quad (24)$$

Torsion is zero at its extremes (when $\kappa = 1$), but nonzero in between.

- Manifesting *initial* congruence with Fig. 2's home frame's world-surface, Fig. 3 surface's initially diagonal outgoing radar trajectories ultimately 'surf' increment curves which are ultimately at 45 degrees to medium curves. Returning counter-directional radar trajectories tend to ultimately 'instantaneously traverse' i.e. practically overlap fixed-τ medium curves at near infinite crossing rate.
- Sharing own-time τ, surface Υ's helical medium curves feature several crucial spatio-temporal characteristics. As geodesics on V_τ *'velocity cylinders'* which in a sense reflect comoving *non-inertial* frames (⇒ Appendix Fig. 4), they are traversed by 'concurrent' radar paths of identical geodesic curvature and at identical crossing angles, *irrespective of differing radar emission times*. Radar trajectory geodesic curvatures, which tend towards zero in the limit since they 'surf' ultimately equatorial increment world-lines, are otherwise nonzero.
- Inter-rocket radar intervals for $L = 0.5548$ and intervals $\Delta\tau = \frac{3\pi}{32}$ on Fig. 2's home frame world-surface, give using (13): $\grave{\tau}_0 - \acute{\tau}_0 = \frac{3\pi}{32}\cdot 3.497$ and $\grave{\tau}_1 - \acute{\tau}_1 = \frac{3\pi}{32}\cdot 4.977$ (as in [17] p.34—Eq. (22)). *The exact same rocket radar intervals are metrically evident in Fig. 3's computer generated own-surface* Υ.

In a recent exemplary book *Differential Geometry of Curves and Surfaces* [16], *Kristopher Tapp* modestly writes in his Introduction: "*...In truth, the most profound application of differential geometry is to modern [relativity] physics, which is beyond the scope of this book.*". Hopefully this sequel paper to [17] will encourage authors of erudite texts such as [16,9] to re-focus spacetime theory maths onto the more proper *Riemannian geometry* domain—without the overgeneralizations of complex variable 'four-vector' parametrizations which, as historically manifest, continue to cause confusion and error at all levels of relativity exposition. This and related matters will be further discussed in a forthcoming book [19].

[16] For the hemix, $\kappa^2 = \Upsilon_{\tau\tau}\cdot\Upsilon_{\tau\tau}$ and $\eta\kappa^2 = [|\Upsilon_\tau\,\Upsilon_{\tau\tau}\,\Upsilon_{\tau\tau\tau}|]$⇒Kreyszig [2] p.34 and p.38.

Acknowledgements

Tribute is due to sadly missed Dunsink Observatory physicist *Ian Elliot* for a decade of helpful advice and encouragement. The MAPLE mathematics software tool [14] has been indispensable in analysing the intricate vector equations. The paper's graphics were produced using specially created software based on the *Persistence of Vision POV-Ray* freeware program [15] (Mac version kindly maintained by *Yvo Smellenbergh*).

Appendix A

A.1. Equations for generator curve Q and surface Υ

Fig. 4 'schematically' envisages our sought after surface in a three-dimensional Euclidean space. The initial medium curve, vertical line *PZ* of the medium's initial 'launch length' *L*, is placed a unit distance above 'origin' point *O*. Each medium increment on *PZ* is associated with its original relative 'launch position' l ($0 \leqslant l \leqslant L$) at its own-time $\tau_0 = 0$.[17] As well as generating helicoid Υ, the rear rocket bottom increment curve *Q* starting at *P* may also generate a smooth *surface of revolution* W_0 swept by rotating it through 2π. An angular segment of W_0 is shown. Note that we do not assume at this point that *surface of revolution* W_0 is necessarily spherical *or even nonplanar* (if planar, W_0 would be *a circular disc*). As also illustrated, surface Υ's respective fixed-τ medium helices traverse vertical cylinders V_τ of height *L* and cylindrical radius *r*. Surface Υ will thus be a helicoid comprising *contiguous intersections of fixed-*τ *concentric cylinders* V_τ *and helicoidally distributed surfaces of revolution* W_l, the latter generated by congruent fixed-l increment τ-curves.

We denote $dr/d\tau$ as $\dot{r}$ and $\partial\Upsilon/\partial\tau$ as Υ_τ etc., spherical radius as *R*, colatitude angle as ϕ and r, θ and z as cylindrical coordinates—*all initially unknown functions of* τ. Keeping in mind that cylindrical coordinate parameters $r = r(\tau)$, $\theta = \theta(\tau)$, $z = z(\tau)$ and factor m is a constant, we write for $0 \leqslant \tau \leqslant \infty$:

$$\text{GENERATOR CURVE} \qquad Q(\tau) = {}_{Cyl}[r, \theta, z] = [r\cos\theta, r\sin\theta, z]. \quad (25)$$

Since curve *Q* traces variable τ, its tangent vector's modulus equals one:

$$\dot{Q} = \left[\dot{r}\cos\theta - r\dot{\theta}\sin\theta, \dot{r}\sin\theta + r\dot{\theta}\cos\theta, \dot{z}\right]. \quad (26)$$

$$\text{UNIT PATH SPEED} \left|\dot{Q}\right|^2 = \dot{Q}\cdot\dot{Q} = \dot{r}^2 + r^2\dot{\theta}^2 + \dot{z}^2 = 1. \quad (27)$$

A.2. Initial conditions

Allocating curve *Q*'s initial direction as *perpendicular* to a 'Greenwich meridian', initial longitude θ_0 will be zero and have initial rate of change $\dot{\theta}_0 = 1$ which (if nonconstant) should by virtue of regularity at least be *monotonic*. As directly evident from Fig. 4's geometry, the *lateral expansion factor* $\partial\lambda/\partial l$ increases smoothly

[17] **Note:** we take the liberty of using subscripts *in three different ways*. (1): Subscripts $_0$ and $_\infty$ denote variables' *limit values*. (2): Subscripts $_\tau$, $_l$, $_\lambda$ denote *tangent and curvature vectors* e.g. $\Upsilon_\tau, \Upsilon_{\tau\tau}$. (3): Subscript $_l$ is used also to denote an increment curve's *surface of revolution* W_l e.g. W_0 for the rear rocket. Similarly, subscript $_\tau$ denotes a fixed-τ *velocity cylinder* V_τ.

from its initial value of *one*, so helicoidally spread increment curves emanate from the initial vertical medium curve *PZ horizontally*.

$$\theta_0 = \phi_0 = 0; \qquad \dot{\theta}_0 = R_0 = 1. \tag{28}$$

A.3. Medium curves' expansion and curvatures

Our fixed $1/m$ pitch factor helicoidal surface may be formulated as:

$$\Upsilon(\tau, l) = [r\cos(\theta + lm), r\sin(\theta + lm), z + l]. \tag{29}$$

Differentiating surface Υ Eq. (29) by l:

$$\Upsilon_l = [-rm\sin(\theta + lm), rm\cos(\theta + lm), 1]; \ \Upsilon_{ll} = -rm^2[\cos(\theta + lm), \sin(\theta + lm), 0]. \tag{30}$$

THE MEDIUM INCREMENTS' EXPANSION FACTOR $\varepsilon(\tau) = \partial\lambda/\partial l$

$$= |\Upsilon_l| = \sqrt{1 + r^2m^2}. \tag{31}$$

Medium curves tangent and curvature vectors are:

$$\Upsilon_\lambda = \Upsilon_l/(\partial\lambda/\partial l) = [-rm\sin(\theta + lm), rm\cos(\theta + lm), 1]/\sqrt{1 + r^2m^2} \tag{32}$$

and

$$\Upsilon_{\lambda\lambda} = \Upsilon_{ll}/(\partial\lambda/\partial l)^2 = [\cos(\theta + lm), \sin(\theta + lm), 0].\frac{-rm^2}{1 + r^2m^2}. \tag{33}$$

Recalling that λ is medium curves *path length parameter* i.e. $\Upsilon_\lambda \cdot \Upsilon_\lambda = 1$, medium helix curves' *principal curvature* is then:

$$M_\kappa = |\Upsilon_{\lambda\lambda}| = \frac{rm^2}{1 + r^2m^2}. \tag{34}$$

Medium expansion (31) and likewise r *increase monotonically with* τ. However principal curvature (34) of each medium helix curve *maximizes* at $rm = 1$. Any *finite* τ changing of medium curve curvature from increasing to decreasing would entail surface Υ having an interim inflection. Hence Υ's coordinate r needs to asymptotically extend towards $1/m$ i.e. as $\tau \to \infty, rm = 1$ and limit expansion factor (31) $\sqrt{1 + r_\infty^2m^2} = \sqrt{2}$. *Medium expansion is limited to the square root of two*. Using (27):

$$r_\infty = \frac{1}{m}, \ \dot{r}_\infty = 0 \qquad \text{and} \qquad \dot{z}_\infty^2 = 1 - \frac{\dot{\theta}_\infty^2}{m^2}. \tag{35}$$

From (29) and (32):

$$\Upsilon_\tau = [\dot{r}\cos(\theta + lm) - r\sin(\tau + lm), \dot{r}\sin(\theta + lm) + r\cos(\theta + lm), \dot{z}], \tag{36}$$

$$\Upsilon_\tau \times \Upsilon_\lambda = \frac{[(\dot{\theta} - \dot{z}m)r\cos(\tau + lm) + \dot{r}\sin(\tau + lm), (\dot{\theta} - \dot{z}m)r\sin(\tau + lm) - \dot{r}\cos(\tau + lm), r\dot{r}m]}{\sqrt{1 + r^2m^2}}$$

and

$$|\Upsilon_\tau \times \Upsilon_\lambda| = \frac{\sqrt{(\dot{\theta} - \dot{z}m)^2 + \dot{r}^2(1 + r^2m^2)}}{\sqrt{1 + r^2m^2}}.$$

(33) and (34) then yield *the normal curvature component* on Υ:

$$M_{\kappa_\Upsilon n} = \frac{\Upsilon_{\lambda\lambda} \cdot (\Upsilon_\tau \times \Upsilon_\lambda)}{|\Upsilon_\tau \times \Upsilon_\lambda|} = \frac{r^2m^2(\dot{\theta} - \dot{z}m)/(1 + r^2m^2)}{\sqrt{\left(\dot{\theta} - \dot{z}m\right)^2 r^2 + \dot{r}^2(1 + r^2m^2)}} = \frac{M_\kappa}{\sqrt{1 + \dot{r}^2m^2/\{M_\kappa.r(\dot{\theta} - \dot{z}m)^2\}}}. \tag{37}$$

A.4. Inverse pitch factor and longitude

(37)'s rightmost denominator term is positive nonzero since $\dot{\theta} > 0$ and $\dot{z}m \leqslant 0$. Hence from (35)ii and (37), as $\dot{r}$ tends towards 0, normal curvature $M_{\kappa_\Upsilon n}$ on surface Υ tends towards principal curvature M_{κ_Υ}. Each such l-helix also lies on a respective V_τ cylinder vertically situated on surface of revolution W_l. Hence as shown in Fig. 5, at V_τ's base point meeting curve Q on W_0, normal vectors of surfaces V_τ and Υ will—as $\tau \to \infty$—be equal i.e. surface Υ *will also then be vertical. Surfaces* Υ *and* W_0 *will tend to 'merge'*. Therefore curve Q becomes horizontal as r tends to its limit value $1/m$ i.e. from (35)iii:

$$\dot{z}_\infty = 0 \qquad \text{and} \qquad \dot{\theta}_\infty = m. \tag{38}$$

From (30)i, (31) and (36), the intersecting medium/increment curves angle cosine is:

$$\iota = \Upsilon_\tau \cdot \Upsilon_l/|\Upsilon_l| = (r^2\dot{\theta}m + \dot{z})/\sqrt{1 + r^2m^2}. \tag{39}$$

From (35), (38) and (39), $\iota_\infty = 1/\sqrt{2}$ i.e. medium curve helices 'in the limit' would be at 45 degrees to ultimately horizontal increment curves. This is reflected by Fig. 5's minuscule triangle where 'in the limit' horizontal increment $\Delta\theta.r_\infty = \Delta lm.1/m = \Delta l$, the latter being a vertical increment on cylinder V_τ.

Hence $\Delta\lambda^2 = \Delta l^2 + \Delta l^2$ and a hypothenuse $\Delta\lambda$ representing a medium helix differential segment relates as $\Delta\lambda = \sqrt{2}\Delta l$. From (31)iii and (35)i we then have:

CONSTANT INVERSE PITCH $m = 1$ and $r_\infty = 1$. (40)

Since $\dot{\theta}_0 = 1$ ((28)ii), $\dot{\theta}_\infty = m = 1$ ((38)ii/(40)i) and since $\dot{\theta}$ may be assumed to be monotonic, we may therefore conclude that *in general* $\dot{\theta} = 1$. Hence:

LONGITUDE EQUALS ARC LENGTH : $\theta = \tau$. (41)

A.5. Spherical coordinates

We now turn to *spherical* parameters R, ϕ, with $r = R\sin\phi$ and $z = R\cos\phi$. Denoting $\frac{d}{d\phi}$ by a dash, we may write $\frac{dr}{d\tau} = \frac{dr}{d\phi} \cdot \frac{d\phi}{d\tau}$ i.e. $\dot{r} = r'\dot{\phi}$ and $\dot{z} = z'\dot{\phi}$.

$$\varepsilon = |\Upsilon_l| = \sqrt{1 + r^2} = \sqrt{1 + R^2(\phi)\sin^2\phi} \qquad \text{and} \tag{42}$$

$$\frac{d\varepsilon}{d\phi} = \frac{d\varepsilon^2}{d\phi}\Big/\frac{d\varepsilon^2}{d\varepsilon} = \frac{2R(\phi)R'(\phi)\sin^2\phi + R^2(\phi)2\sin\phi\cos\phi}{2\varepsilon} = (R'(\phi)\sin\phi + z)\frac{r}{\varepsilon}. \tag{43}$$

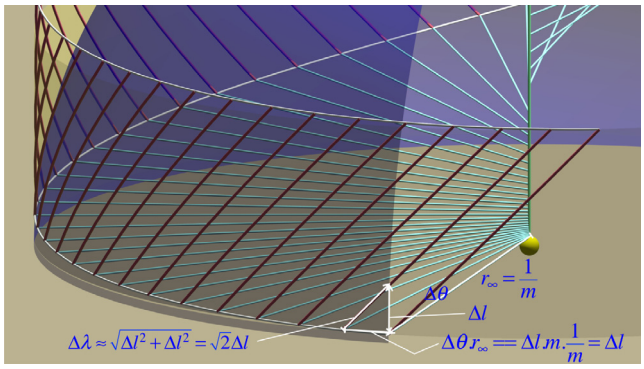

Fig. 5. Medium expansion in the limit.

Curve Q in the limit becomes horizontal on W_0, so $R'(\phi_\infty)$ and $\frac{d\varepsilon}{d\phi}|_\infty$ are zero. From (40) and (31) $r_\infty/\varepsilon_\infty = \frac{1}{\sqrt{2}}$ so (43) implies $z_\infty = 0$ i.e. $\phi_\infty = \pi/2$.

$$R_\infty = R_\infty \sin\phi_\infty = r_\infty = 1. \tag{44}$$

Generator curve Q's surface of rotation W_0 will, like Υ, not have an inflection point, so it is reasonable to assume that its spherical radius R will be monotonic just like its cylindrical radius r. Since from (28) iv $R(\phi_0) = 1$, (44) iii means R must be *constant*.

Surfaces of revolution W_l are unit radius hemispheres. (45)

Since $r = \sin\phi$ and $z = \cos\phi$, therefore $\dot{r} = r'\dot{\phi} = \cos\phi.\dot{\phi}$ and $\dot{z} = z'\dot{\phi} = -\sin\phi.\dot{\phi}$. Hence as $\theta = \tau$, from (27) iii: $\cos^2\phi.\dot{\phi}^2 + \sin^2\phi + \sin^2\phi.\dot{\phi}^2 = 1$ i.e. $\dot{\phi}^2 = 1 - \sin^2\phi$ and $\cos\phi = \dot{\phi} = \frac{d\phi}{d\tau}$ so $\tau = \int_0^\phi \frac{d\phi}{\cos(\phi)}$. This solves as

The Gudermann function : $\phi = gd(\tau) = arcsin(\tanh\tau)$.

Hence $r = \sin\phi = \tanh\tau$ and $z = \cos\phi = \sqrt{1 - \tanh^2\tau} = \frac{1}{\cosh\tau}$.

$$\text{Generator curve Q} = \left[\tanh\tau\cos\tau, \tanh\tau\sin\tau, \frac{1}{\cosh\tau}\right]. \tag{46}$$

The generator *'hemix'* curve Q is uniquely identified as hemispherical with path length τ equal to traversed longitude θ. Unit pitch factor $1/m$ then uniquely establishes helicoidal surface Υ which we designate as a *'hemicoid'*.

References

[1] Loedel EP. Aberraciôn y Relatividad Anales de la Sociedad Científica Argentina 1948;145:3.
[2] Kreyszig E. Differential geometry dover. Univ. of Toronto Press; 1959, 1991.
[3] Dewan E, Beran M. Note on stress effects due to relativistic contraction. Am J Phys 1959;27:517–8.
[4] Bell JS. How to teach special relativity in Speakable and Unspeakable in Quantum Mechanics: p. 67–80. Camb.U.P. 1976/1987.
[5] Desloge D, Philpott R. Uniformly accelerated reference frames in special relativity. Am J Phys 1987;55:252–61.
[6] Brown H, Pooley O. Minkowski spacetime: a glorious non-entity British Journal for the Philosophy of Science. Also 2006 in The Ontology of Spacetime Elsevier http://philsci-archive.pitt.edu/1661/1/Minkowski.pdf. 2004.
[7] Rindler W. Relativity, Special, General and Cosmological Oxford U.P. Exercise 3.24 (incorrect): A certain piece of elastic breaks when it is stretched to twice its unstretched length. At time $t = 0$, all points of it are accelerated longitudinally with constant proper acceleration α, from rest in the unstretched state. Prove that the elastic breaks at $t = \sqrt{3}c/\alpha$ [when $\gamma = 2$]. 2001, 2006.
[8] Franklin J. Lorentz contraction, Bell's spaceships and rigid body motion in special relativity Eur. J. Phys. 31 291–298 Page 294 (incorrect): a cable connecting the two ships would snap when $d' = \gamma.d = d_{max}$. 2010.
[9] Pressley A. Elementary differential geometry. Springer; 2010.
[10] Podosenov S, Foukzon J, Potapov A. A study of the motion of a relativistic continuous medium. Gravitation Cosmol 2010;16(4):307–12. Pleiades/Springer Moscow.
[11] Coleman B. Relativity Acceleration's Cosmographicum and its Radar Photon Surfings—A Euclidean Diminishment of Minkowski Spacetime. http://www.dpg-verhandlungen.de/year/2012/conference/goettingen/part/gr/session/4/contribution/4. 2012.
[12] Podosenov S, Potapov A, Foukzon J, Menkova E. Geometry of noninertial bases in relativistic mechanics of continua and Bell's problem solution. Int J Recent Adv Phys (IJRAP) 2014;3(1):23–37. http://wireilla.com/physics/ijrap/papers/3114ijrap04.pdf.
[13] Redžić DV. Relativistic length agony continued Serb. Astron J 2014;188:55–65. http://www.doiserbia.nb.rs/Article.aspx?ID=1450-698X1488055R.
[14] Maple. Mathematical software tool Maplesoft Ontario Canada; 2016.
[15] Raytracer Pty. Ltd., Victoria Australia 2016 POV-Ray—Persistence of Vision Ray-tracing software tool http://www.povray.org.
[16] Tapp K. Differential geometry of curves and surfaces. Springer; 2016.
[17] Coleman B. Minkowski spacetime does not apply to a homogeneously accelerating medium. Results Phys 2016;6:31–8. http://www.sciencedirect.com/science/article/pii/S2211379716000024.
[18] Podosenov S, Foukzon J, Menkova E. Structure equations, permitted movement of relativistic continuum and Sagnac's, Erenfest's and Bell's Paradoxes. Phys Sci Int J 2017;13(2):1–18. http://www.journalrepository.org/media/journals/PSIJ_33/2017/Jan/Podosenov1322016PSIJ30616.pdf.
[19] Coleman B. Spacetime Fundamentals Intelligibly (Re)Learnt—Special Relativity's Cosmographicum Textbook to be published October 2017; 2017.